Naturally Fractured Reservoirs

Shape Factor

Shahab Gerami, Fall 2010

Well Test Analysis on the Basis of Warren & Root Model

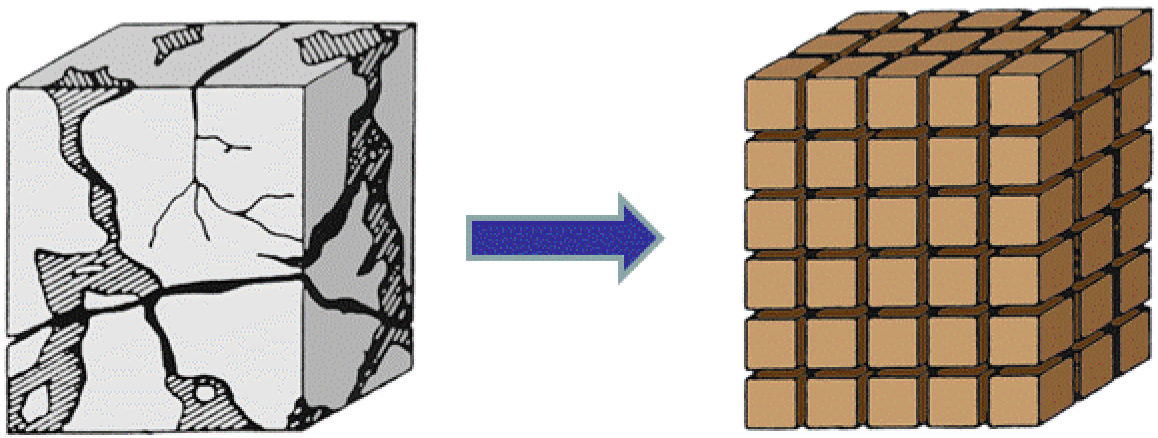

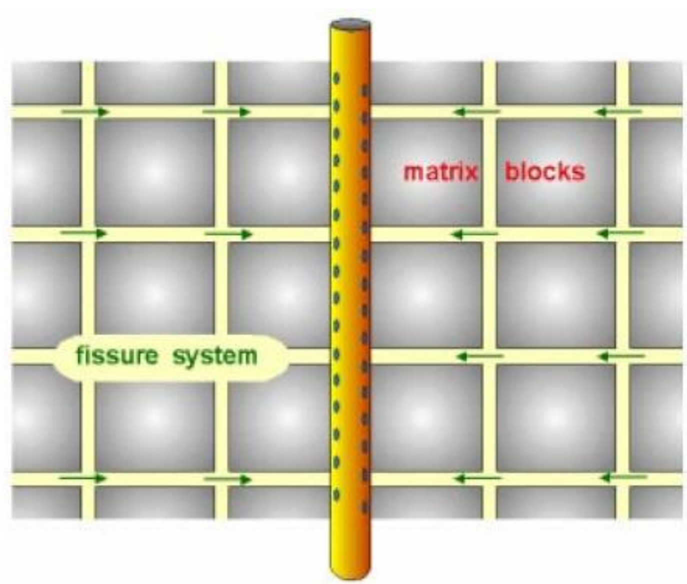

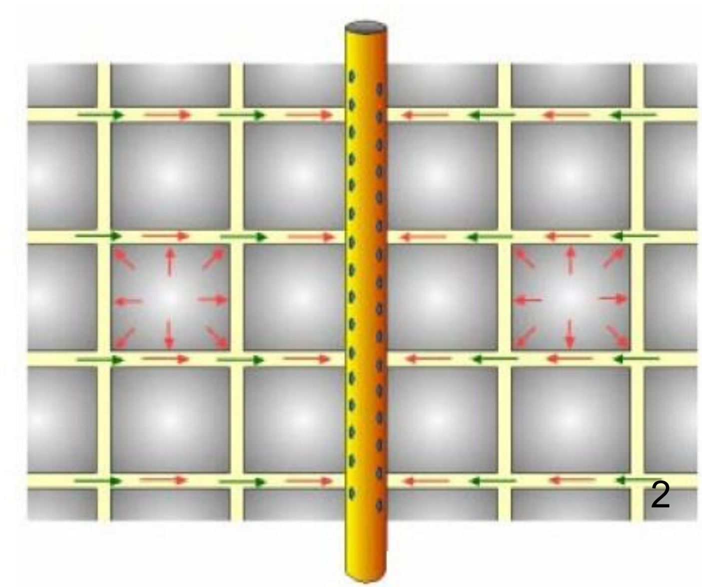

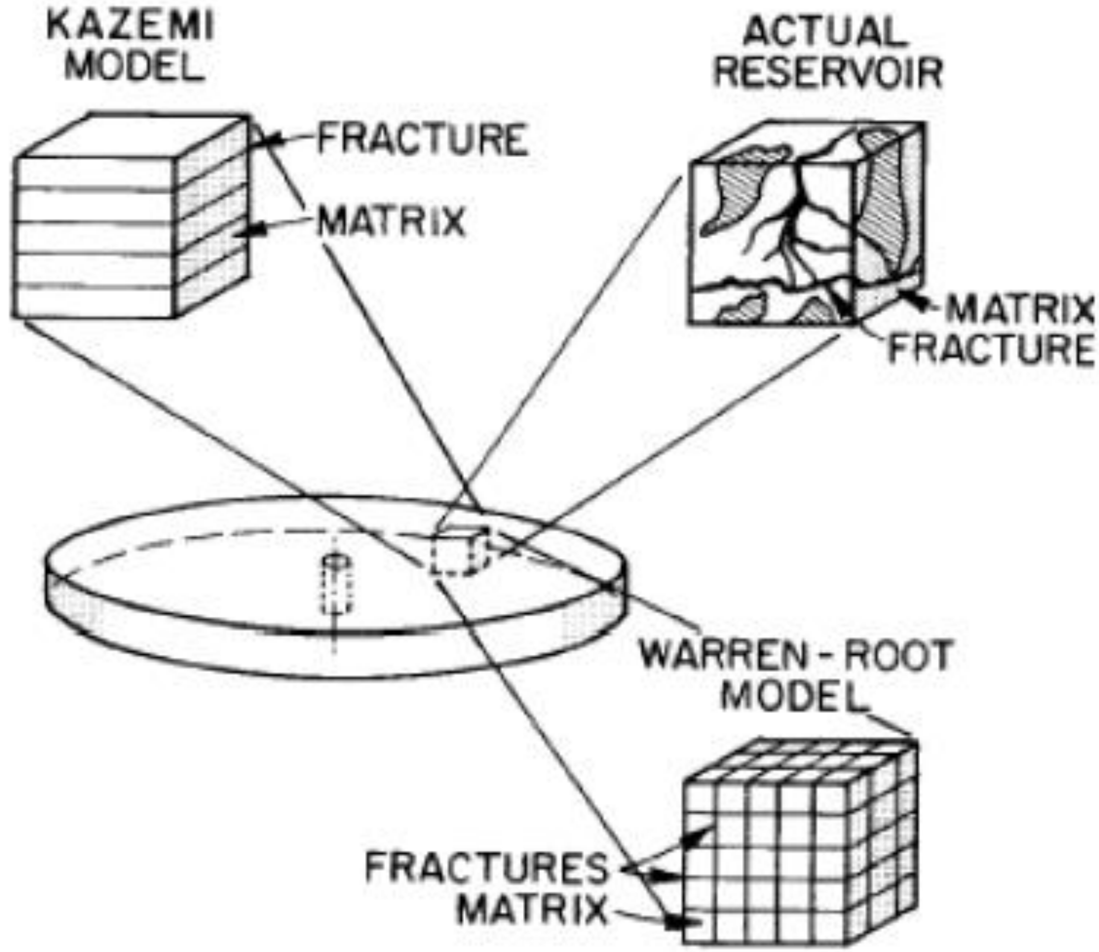
KAZEMI
MODEL
FRACTURE
MATRIX
ACTUAL
RESERVOIR
MATRIX
FRACTURE
WARREN - ROOT
MODEL
FRACTURES
MATRIX

Important Features of Some Mathematical Models Describing Flow from Matrix to Fracture

Warren and Root (1965)

- Analytical model.
- Pseudo-steady state model.
- Matrix flux is independent of a spatial position and is proportional to the pressure difference between matrix and fracture.
- Simplifying the mathematical analysis of the flow problem.
- S-shaped transitional curve with an inflection point.
- The separation of the two parallel lines allows calculation of the storativity ratio.

Kazemi (1969)

- Numerical model.
- Unsteady state model.
- Linear transitional curve with no inflection point.

de Swaan (1976)

- Analytical model.
- Unsteady state model.
- A convolution theorem gives the relationship between the source term and the pressure in the fracture medium.
- Linear transitional curve with no inflection point.

Najurieta (1980)

- Analytical model.
- Unsteady state model.
- Approximate solution to de Swaan model.
- Only applicable for transient period (no boundary dominated period).
- Linear transitional curve with no inflection point.

Streltsova (1983)

- Analytical model.
- Pressure gradient model.
- Matrix flux is proportional to the averaged pressure gradient throughout the matrix block.
- Linear transitional curve with no inflection point.

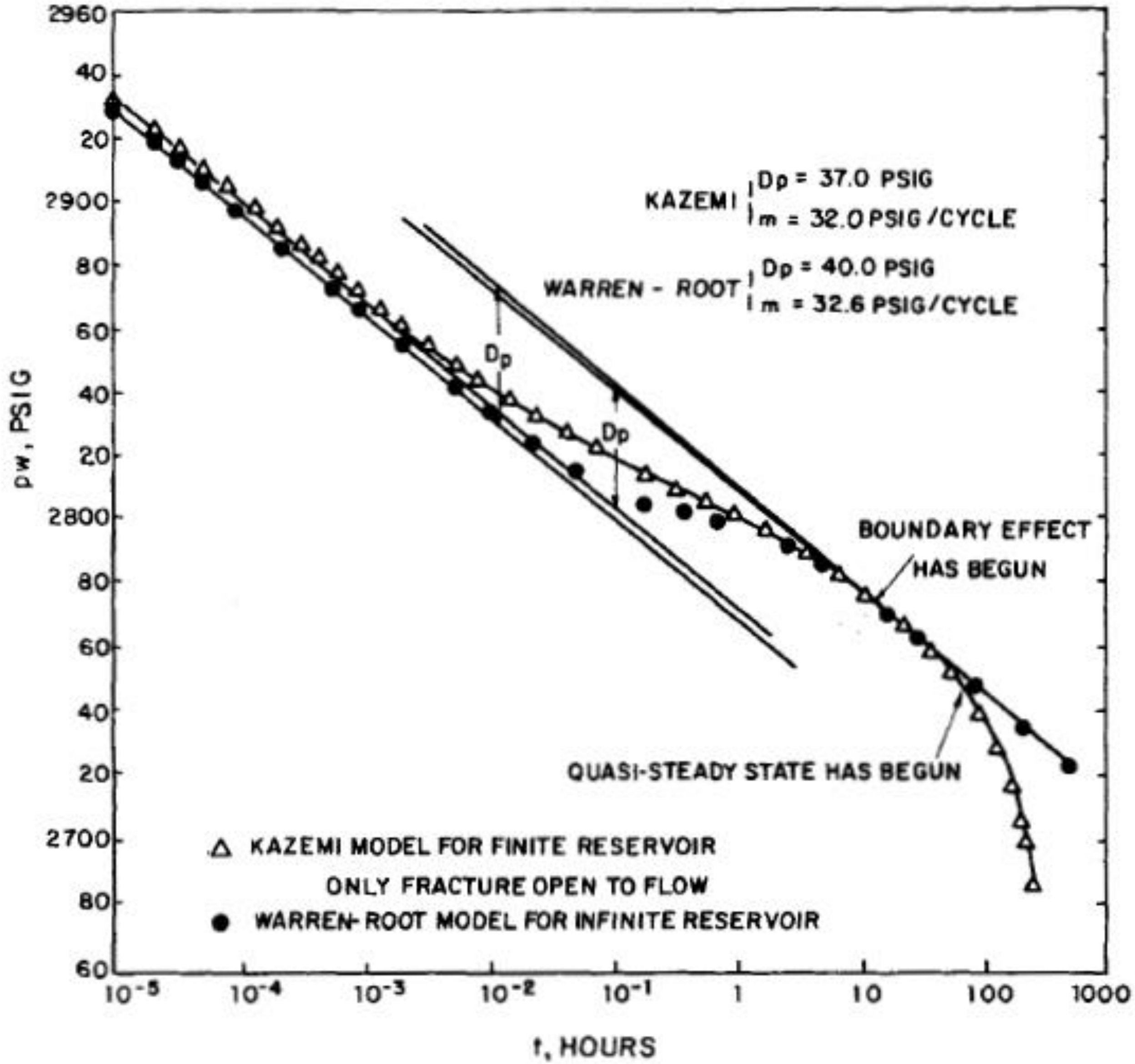

Fig. 2-9. Wellbore pressure solution as given by Kazemi's model and comparison with Warren and Root's model (after Kazemi, 1969). Duration of the first semi-log straight line is shorter as predicted by Kazemi's model. Courtesy of SPE-AIME.

MODEL BY KAZEMI

Kazemi (1969) formulated a radial, numerical model for a well producing from a finite drainage area. The model consisted of matrix and horizontal fractures (Figure 6-8). Flow in the model was three dimensional and unsteady state, but the fluid entered the wellbore only through the fractures.

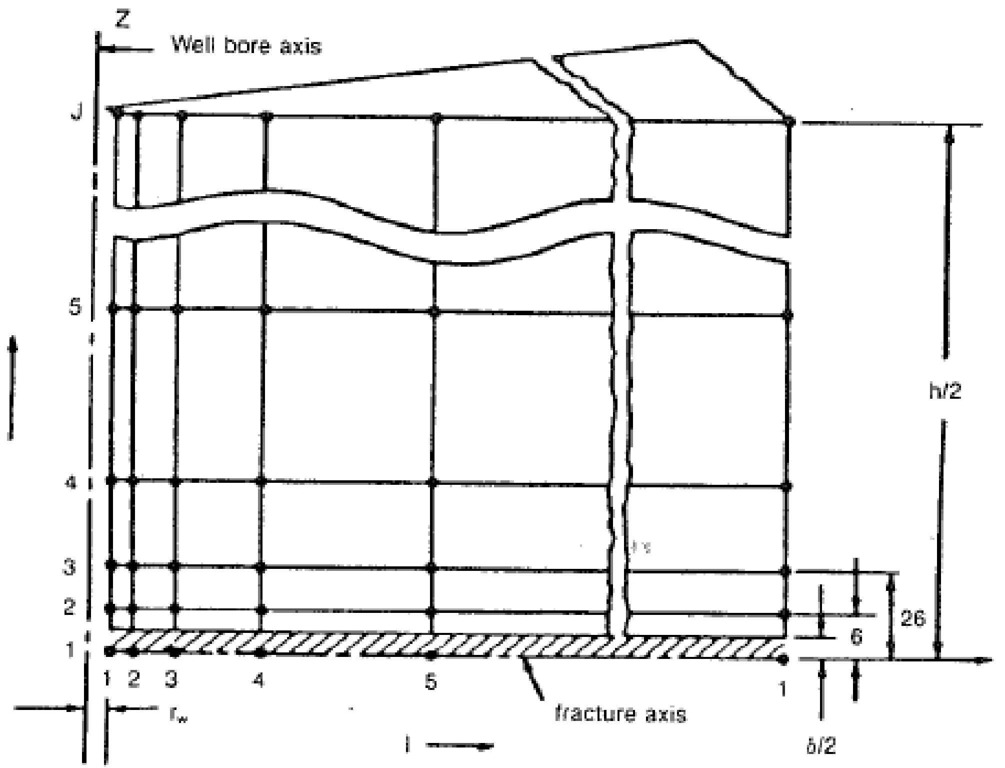

Figure 6-8. Grid for mesh points for ADI procedure. Copyright © SPE, Kazemi, *SPEJ*, Dec. 1969 [8].

Based on this model, Kazemi reached the following conclusions:

1. If the drainage boundary effects are not sensed during the test and $k_m h_m << k_f h_f$ such that $\lambda < 5 \times 10^{-5}$ and Δp (see Figure 6-3) is greater than 100 psi, and if it is possible to produce the well at a constant rate from the instant of opening the well to flow, then the slope, m, and the pressure difference, Δp, would yield accurate estimates of $k_f h_t$ and ω as predicted by the theory developed by Warren and Root. However, because the duration of the first straight line is very short, it is unlikely that the first straight line would develop under actual field test conditions, thus ω cannot be calculated in practice from a drawdown test. Calculation of $k_f h_t$ and ω from a buildup test would be possible if wellbore storage effects are negligible. If $\lambda > 5 \times 10^{-5}$, the duration of the first straight line would be extremely short such that it may not be observed under real field conditions.

2. If the drainage boundary effects are sensed during the test, then the second straight line would not be parallel to the first, and ω cannot be calculated. But $k_f h_t$ can be estimated from the slope, m, of the first straight line. In the event that the first straight line is obscured by wellbore storage effects, the use of the slope of the second straight line would overestimate the flow capacity, $k_f h_t$.
3. The time to reach the semi-steady state, t_{pss}, is given by:

$$t_{pss} = 1{,}580 \frac{(\phi_m + \phi_f)\ \mu\ C_t\ r_e^2}{k_f} \tag{6-13}$$

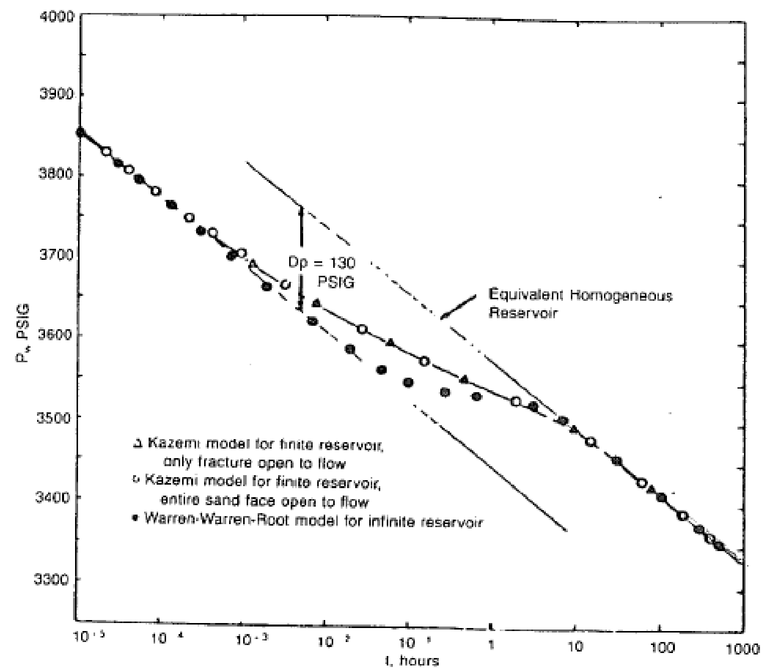

Shape Factor

Calculation of fluid transfer calculation between the matrix and fracture network needs knowledge of:

- ➢Matrix and fracture porosity,
- ➢Matrix and fracture permeability,
- ➢Matrix and fracture compressibility,
- ➢Shape factor

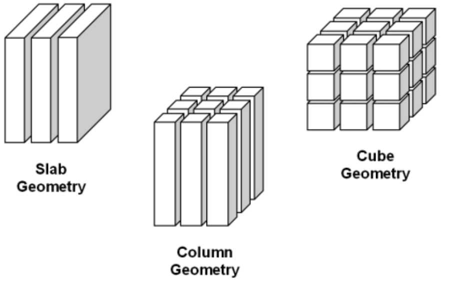

Shape factor is often represented by the symbol '**σ** ' in units of ft^{-2} . This term is best understood from the Warren and Root paper (1963) in which they idealized the system as a stack of "sugar-cubes".

➢There has been much discussion about the physical meaning and the functional form of the shape factor.

➢From a practical view, it is a second order, distance-related, geometric parameter that is used to calculate the mass transfer coefficient between matrix blocks and surrounding fractures.

➢Shape factor is a function of fracture spacing (or intensity), and is not inherently a time-dependent parameter, but several authors have attempted to treat it as such.

The pseudo-steady state, **analytically** derived expression for the shape factor (Kazemi and Gilman, 1993, Chang, 1993, Zimmerman, 1993, Lim, 1995) in terms of **fracture spacing** (L) in the x, y, and z directions is:

$$\sigma = \pi^2 \left(\frac{1}{L_x^{\ 2}} + \frac{1}{L_y^{\ 2}} + \frac{1}{L_z^{\ 2}} \right)$$

The pseudo-steady state, **numerically** derived expression for shape factor (Kazemi, 1976, Kazemi and Gilman, 1988) has a coefficient of **4** rather than **Π**.

Transport in Porous Media (2006) 64: 51–71
DOI 10.1007/s11242-005-1398-x

Effects of Fracture Boundary Conditions on Matrix-fracture Transfer Shape Factor

HASSAN HASSANZADEH and MEHRAN POOLADI-DARVISH*
Department of Chemical & Petroleum Engineering, University of Calgary, 2500 University Drive NW, Calgary, AB, Canada T2N 1N4

This study shows that for a single-phase flow in a particular matrix block, the shape factor that Warren and Root defined is not unique and depends on the pressure in the fracture and how it changes with time.

Dual Porosity Models

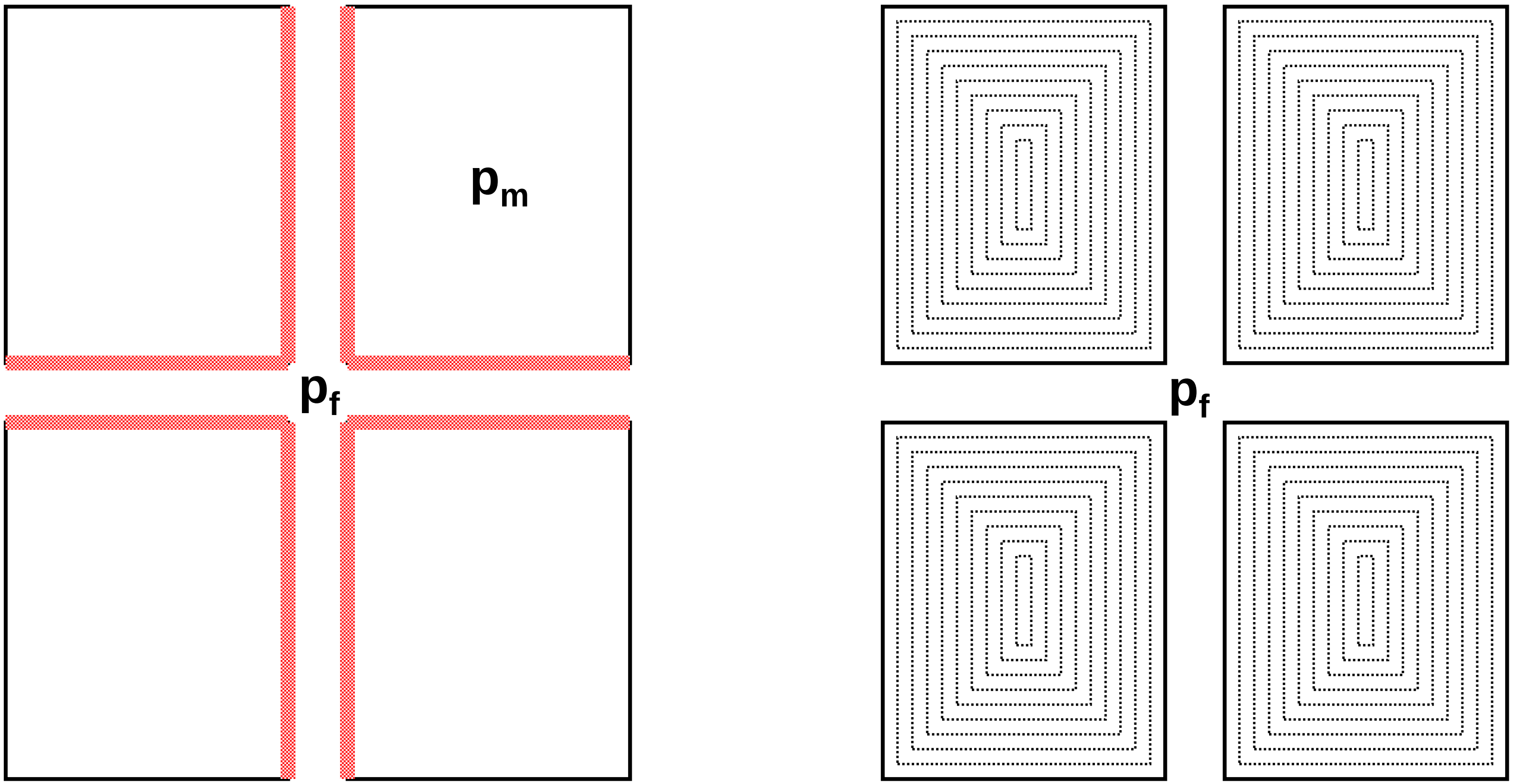

Pseudosteady State **Transient**

Pseudo-steady state (PSS) Transfer Model

$$Q_{\mathrm{m}} = \frac{k_{\mathrm{m}}\rho}{\mu}\sigma\left(\overline{p}_{\mathrm{m}} - p_{\mathrm{f}}\right), \quad (1)$$

$$Q_{\mathrm{m}} = -\phi_{\mathrm{m}} c_{\mathrm{m}} \rho \left(\frac{\partial \overline{p}_{\mathrm{m}}}{\partial t}\right), \quad (2)$$

p_{f}	pressure $[M/LT^2]$
$\overline{P}_{\mathrm{m}}$	average matrix pressure in Laplace domain
Q_{m}	matrix-fracture exchange term $[M/L^3T]$
ρ	fluid density $[M/L^3]$
σ	shape factor constant $[1/L^2]$

The PSS model does not account for the pressure transient within the matrix.

Transient Transfer Model

➢This type of model is called a "transient transfer model" and does not use the matrix-fracture transfer shape factor.

$$\nabla^2 p_{\mathrm{m}} = \frac{1}{\eta_{\mathrm{m}}} \left(\frac{\partial p_{\mathrm{m}}}{\partial t} \right), \tag{3}$$

$$\eta_{\mathrm{m}} = k_{\mathrm{m}} / \phi \mu c_{\mathrm{m}}$$

the matrix hydraulic diffusivity

➢In the transient model, the fluid transfer rate between the matrix and fracture is proportional to the pressure gradient at the matrix block surface as given by:

$$Q_{\mathrm{m}} = \frac{A k_{\mathrm{m}} \rho}{\mu V_{\mathrm{m}}} \nabla p_{\mathrm{m}} |_{\mathrm{matrix\ \ face}}, \tag{4}$$

Petroleum engineering literature shows that the shape factor remains a controversial topic. A large body of research in the area of naturally fractured reservoirs simulation is devoted to representing an accurate matrix fracture exchange term (Kazemi et al., 1976; Thomas et al., 1983; Kazemi and Gilman, 1993; Lim and Aziz, 1995; Quintard and Whittaker, 1996; Noetinger and Estebenet, 1998; Bourbiaux et al., 1999; Coats, 1999; Noetinger et al., 2000; Penuela et al., 2002a,b; Sadra et al., 2002).

The shape factor is usually derived from a simple mechanism of pressure diffusion with constant fracture pressure as a boundary condition, whereas the physical exchange mechanism in fractured reservoirs is more complex.

To investigate the boundary condition dependency of shape factor, the diffusivity equation is solved analytically in Laplace domain for different depletion regimes in the fracture including:

1. constant flux at a matrix-fracture interface,
2. exponential depletion, and
3. linear pressure depletion schemes.

Shape Factor- Literature Review

1. Barenblatt et al. (1960) introduced the classic dual porosity concept in the early 1960s.

2. Warren and Root (1963) applied this concept to reservoir engineering, principally for well testing applications. They used a geometrical approach to derive the shape factors for one, two, and three sets of orthogonal fractures.

3. Kazemi et al. (1976) introduced the shape factor in double porosity simulators. They obtained shape factors by discretization of pressure equation for single-phase flow using the standard seven point finite difference. Since then, this shape factor formulation has been used in standard reservoir simulators.

4. Thomas et al. (1983) presented another expression for the shape factor that was validated by multiphase flow numerical simulations.

Lim and Aziz (1995) suggested that the shape factor depends on the geometry and physics of pressure diffusion in the matrix. Here, Hassanzadeh and Pooladi-Darvish showed that the shape factor also depends on the way the pressure changes in the fracture.

Table I. Summary of the shape factor constants σL^2 found in literature

Investigator(s)	Approach	Fluid flow	1D	2D	3D	Transient/ PSS*
Warren and Root (1963)	Geometrical	Single phase	12	32	60	PSS
Kazemi *et al.* (1976)	Numerical	Single phase	4	8	12	PSS
Thomas *et al.* (1983)	Numerical	Two phase	–	–	25	Transient
Coats (1999)	Analytical	Single phase	12	28.45	49.58	PSS
Coats (1999)	Numerical	Two phase	8	16	24	PSS
Kazemi and Gilman (1993)	Analytical	Single phase	–	–	29.61	Transient
Lim and Aziz (1994)	Analytical	Single phase	9.87	19.74	29.61	Transient
Quintard and Whitaker (1996)	Averaging	Single phase	12	28.4	49.6	
Bourbiaux *et al.* (1999)	Numerical	Single phase	–	20	–	PSS
Noetinger *et al.* (2000)	Random walk	Single phase	11.5	27.1	–	
Penuela *et al.* (2002)	Numerical	Two phase	9.87	–	–	Transient
Sarda *et al.* (2002)	Numerical	Single phase	8	24	48	Transient

*Pseudo-steady state transfer model.

Methodology

Combining Equations (1) and (2) leads to the definition of the single-phase shape factor

$$Q_{\mathrm{m}} = \frac{k_{\mathrm{m}}\rho}{\mu}\sigma\left(\overline{p}_{\mathrm{m}} - p_{\mathrm{f}}\right), \quad (1)$$

$$Q_{\mathrm{m}} = -\phi_{\mathrm{m}} c_{\mathrm{m}} \rho \left(\frac{\partial \overline{p}_{\mathrm{m}}}{\partial t}\right), \quad (2)$$

⬇

$$\sigma = -\left(\frac{\partial \overline{p}_{\mathrm{m}}}{\partial t}\right)\frac{1}{\eta_{\mathrm{m}}\left(\overline{p}_{\mathrm{m}} - p_{\mathrm{f}}\right)}. \quad (5)$$

Determination of $\mathbf{p_m}$ in Equation (5) requires solution of the matrix pressure subject to the appropriate initial and boundary conditions. The governing partial differential equation that describes the single-phase pressure diffusion in a matrix block is given by Equation (3).

$$\nabla^2 p_{\mathrm{m}} = \frac{1}{\eta_{\mathrm{m}}} \left(\frac{\partial p_{\mathrm{m}}}{\partial t} \right), \tag{3}$$

This equation can be solved by the Laplace transform method with an arbitrary boundary condition. The Laplace domain solution for matrix pressure $P_m(x, s)$, can then be integrated to obtain the average matrix block pressure in the Laplace domain $P_m(s)$, as given below:

$$\overline{P}_{\mathrm{m}} = \frac{1}{V_{\mathrm{m}}} \int_{V_{\mathrm{m}}} P_{\mathrm{m}} \,\mathrm{d} V_{\mathrm{m}}, \tag{6}$$

$$\ell \left\{ \frac{\partial \overline{p}_{\mathrm{m}}}{\partial t} \right\} = s' \overline{P}_{\mathrm{m}} - \overline{p}_{\mathrm{m}}(0). \tag{7}$$

$$\sigma = \frac{\ell^{-1} \left\{ s' \overline{P}_{\mathrm{m}} - \overline{p}_{\mathrm{m}}(0) \right\}}{\eta_{\mathrm{m}} \left\{ \ell^{-1} \left(\overline{P}_{\mathrm{m}} \right) - p_f \right\}}. \tag{8}$$

Solutions

Consider a **slab shape matrix block** of thickness $\mathbf{h_m}$, with initial pressure $\mathbf{p_i}$ sandwiched by two parallel planes of fractures with pressure $\mathbf{p_f}$ where in general $\mathbf{p_f}$ can be a function of time. The governing partial differential equation and its associated initial and boundary conditions are given by:

$$\frac{\partial^2 \Delta p_m}{\partial x_D^2} = \frac{\partial \Delta p_m}{\partial t_D}, \tag{9}$$

Constant boundary condition

$$\Delta p_m(x_D, t_D) = 0, \quad t_D = 0, \quad 0 \le x_D \le 1,$$

$$\Delta p_m(x_D, t_D) = \Delta p_f, \quad t_D > 0, \quad x_D = 1,$$

$$\frac{\partial \Delta p_m(x_D, t_D)}{\partial x_D} = 0, \quad t_D > 0, \quad x_D = 0,$$

No flow boundary condition

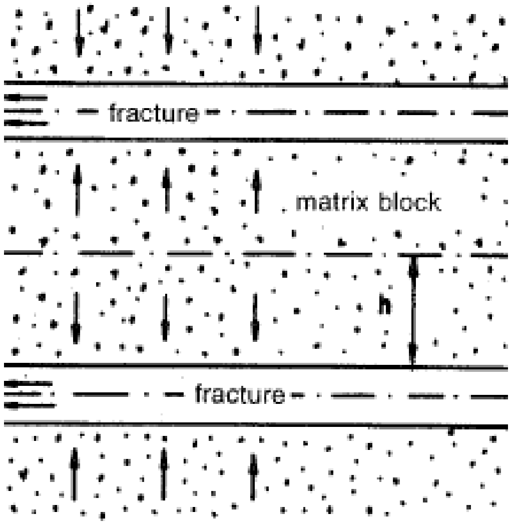

where

$$\Delta p = p(x_D, t_D) - p_i.$$

$$x_D = x / l_c \quad \text{and} \quad t_D = \eta_m t / l_c^2, \tag{10}$$

For a **slab shaped matrix** block we consider **half of** the matrix-block thickness as the characteristic length.

$$\Delta P_{\mathrm{m}} = \frac{1}{\eta_{\mathrm{m}}} \left(\frac{h_{\mathrm{m}}}{2} \right)^2 \frac{\Delta p_{\mathrm{f}} \cosh(x_{\mathrm{D}} \sqrt{s})}{s \cosh \sqrt{s}}, \tag{11}$$

s	laplace variable with respect to t_{D}
s'	laplace variable with respect to t
t	time $[T]$
t_{D}	dimensionless time

$$\overline{P}_{\mathrm{m}} = \frac{1}{V_{\mathrm{m}}} \int_{V_{\mathrm{m}}} P_{\mathrm{m}} \, \mathrm{d} V_{\mathrm{m}},$$

$$\Delta \overline{P}_{\mathrm{m}} = \frac{1}{\eta_{\mathrm{m}}} \left(\frac{h_{\mathrm{m}}}{2} \right)^2 \frac{\Delta p_{\mathrm{f}} \tanh \sqrt{s}}{s \sqrt{s}}. \tag{12}$$

Before we substitute for $\mathbf{P_m}$ in Equation (8), we need to distinguish between the Laplace transform parameters when transform is taken with respect to **t** and when taken with respect to $\mathbf{t_D}$ called **s'** and **s**, respectively

$$s' = \left(\eta_m / l_c^2\right) s$$

$$\sigma h_m^2 = -\frac{4\ell^{-1}\{s\,\Delta\overline{P}_m\}}{\left\{\ell^{-1}\{\Delta\overline{P}_m\} - \Delta p_f\right\}}. \qquad (13)$$

Equation (12) can be incorporated in Equation (13) to obtain

$$\sigma h_m^2 = \frac{\ell^{-1}\left\{\frac{\tanh\sqrt{s}}{\sqrt{s}}\right\}}{\left\{\frac{\eta_m}{h_m^2} - \frac{1}{4}\ell^{-1}\left\{\frac{\tanh\sqrt{s}}{s\sqrt{s}}\right\}\right\}}. \qquad (14)$$

The product group σh_m^2 is dimensionless and will be called shape factor.

Governing Equation

$$\frac{\partial^2 \Delta p_{\mathrm{m}}}{\partial x_{\mathrm{D}}^2} = \frac{\partial \Delta p_{\mathrm{m}}}{\partial t_{\mathrm{D}}}$$

$$x_{\mathrm{D}} = x/l_{\mathrm{c}} \quad \text{and} \quad t_{\mathrm{D}} = \eta_{\mathrm{m}} t/l_{\mathrm{c}}^2$$

IC & BCs

$$\Delta p_{\mathrm{m}}(x_{\mathrm{D}}, t_{\mathrm{D}}) = 0, \qquad t_{\mathrm{D}} = 0, \quad 0 \le x_{\mathrm{D}} \le 1$$

$$\Delta p_{\mathrm{m}}(x_{\mathrm{D}}, t_{\mathrm{D}}) = \Delta p_{\mathrm{f}}, \qquad t_{\mathrm{D}} > 0, \quad x_{\mathrm{D}} = 1,$$

$$\frac{\partial \Delta p_{\mathrm{m}}(x_{\mathrm{D}}, t_{\mathrm{D}})}{\partial x_{\mathrm{D}}} = 0, \qquad t_{\mathrm{D}} > 0, \quad x_{\mathrm{D}} = 0,$$

Table II. Matrix pressure and its average in slab shape for different boundary conditions

Matrix and fracture BC	P_{m}	$\overline{P}_{\mathrm{m}}$
Constant pressure p_{f}	$\frac{1}{\eta_{\mathrm{m}}}\left(\frac{h_{\mathrm{m}}}{2}\right)^2\left[\frac{p_{\mathrm{i}}}{s}+\frac{\cosh(x_{\mathrm{D}}\sqrt{s})}{s\cosh\sqrt{s}}\right]$	$\frac{1}{\eta_{\mathrm{m}}}\left(\frac{h_{\mathrm{m}}}{2}\right)^2\left[\frac{p_{\mathrm{i}}}{s}+\frac{(p_{\mathrm{f}}-p_{\mathrm{i}})\tanh\sqrt{s}}{s\sqrt{s}}\right]$
Linear decline, $p_{\mathrm{f}} = p_{\mathrm{i}}(1-\alpha t)\alpha \leqslant 1/t$	$\frac{1}{\eta_{\mathrm{m}}}\left(\frac{h_{\mathrm{m}}}{2}\right)^2\left[\frac{p_{\mathrm{i}}}{s}-\frac{p_{\mathrm{i}}}{s^2}\frac{\alpha\cosh(x_{\mathrm{D}}\sqrt{s})}{\cosh(\sqrt{s})}\right]$	$\frac{1}{\eta_{\mathrm{m}}}\left(\frac{h_{\mathrm{m}}}{2}\right)^2\left[\frac{p_{\mathrm{i}}}{s}-\frac{p_{\mathrm{i}}}{s^2\sqrt{s}}\alpha\tanh\sqrt{s}\right]$
Exponential, $p_{\mathrm{f}} = p_{\mathrm{i}}\mathrm{e}^{-\alpha t}$	$\frac{1}{\eta_{\mathrm{m}}}\left(\frac{h_{\mathrm{m}}}{2}\right)^2\left[\frac{p_{\mathrm{i}}}{s}-p_{\mathrm{i}}\left(\frac{1}{s}-\frac{1}{s+\alpha}\right)\left(\frac{\cosh(x_{\mathrm{D}}\sqrt{s})}{\cosh(\sqrt{s})}\right)\right]$	$\frac{1}{\eta_{\mathrm{m}}}\left(\frac{h_{\mathrm{m}}}{2}\right)^2\left[\frac{p_{\mathrm{i}}}{s}-\frac{p_{\mathrm{i}}}{s\sqrt{s}}\left(1-\frac{s}{s+\alpha}\right)\tanh\sqrt{s}\right]$
Constant flux, Q_{m}	$\frac{1}{\eta_{\mathrm{m}}}\left(\frac{h_{\mathrm{m}}}{2}\right)^2\left[\frac{p_{\mathrm{i}}}{s}-\frac{Q_{\mathrm{m}}\mu h_{\mathrm{m}}^2}{4\rho k_{\mathrm{m}}}\frac{\cosh(x_{\mathrm{D}}D\sqrt{s})}{s\sqrt{s}\sinh\sqrt{s}}\right]$	$\frac{1}{\eta_{\mathrm{m}}}\left(\frac{h_{\mathrm{m}}}{2}\right)^2\left[\frac{p_{\mathrm{i}}}{s}-\left(\frac{h_{\mathrm{m}}^2\mu}{4k_{\mathrm{m}}\rho}\right)\frac{Q_{\mathrm{m}}}{s^2}\right]$

Table III. Matrix pressure and its average in cylindrical shape for different boundary conditions

Matrix and fracture BC	P_{m}	$\overline{P}_{\mathrm{m}}$
Constant pressure p_{f}	$\frac{R_{\mathrm{m}}^2}{\eta_{\mathrm{m}}}\left[\frac{p_{\mathrm{i}}}{s}+\frac{(p_{\mathrm{f}}-p_{\mathrm{i}})}{s}\frac{I_0(r\sqrt{s})}{I_1(R_o\sqrt{s})}\right]$	$\frac{R_{\mathrm{m}}^2}{\eta_{\mathrm{m}}}\left[\frac{p_{\mathrm{i}}}{s}+\frac{(p_{\mathrm{f}}-p_{\mathrm{i}})}{s\sqrt{s}}\frac{2I_0(\sqrt{s})}{I_1(\sqrt{s})}\right]$
Linear decline, $p_{\mathrm{f}}=p_{\mathrm{i}}(1-\alpha t)\alpha\leqslant 1/t$	$\frac{R_{\mathrm{m}}^2}{\eta_{\mathrm{m}}}\left[\frac{p_{\mathrm{i}}}{s}-\frac{p_{\mathrm{i}}}{s^2}\frac{\alpha I_0(r_{\mathrm{D}}\sqrt{s})}{I_1(\sqrt{s})}\right]$	$\frac{R_{\mathrm{m}}^2}{\eta_{\mathrm{m}}}\left[\frac{p_{\mathrm{i}}}{s}-\frac{2\alpha p_{\mathrm{i}}}{s^2\sqrt{s}}\frac{I_0(\sqrt{s})}{I_1(\sqrt{s})}\right]$
Exponential, $p_{\mathrm{f}}=p_{\mathrm{i}}\mathrm{e}^{-\alpha t}$	$\frac{R_{\mathrm{m}}^2}{\eta_{\mathrm{m}}}\left[\frac{p_{\mathrm{i}}}{s}-p_{\mathrm{i}}\left(\frac{1}{s}-\frac{1}{s+\alpha}\right)\frac{I_0(r_{\mathrm{D}}\sqrt{s})}{I_1(\sqrt{s})}\right]$	$\frac{R_{\mathrm{m}}^2}{\eta_{\mathrm{m}}}\left[\frac{p_{\mathrm{i}}}{s}-\frac{p_{\mathrm{i}}}{s}\left(1-\frac{s}{s+\alpha}\right)\frac{2}{\sqrt{s}}\frac{I_0(\sqrt{s})}{I_1(\sqrt{s})}\right]$
Constant flux, Q_{m}	$\frac{R_{\mathrm{m}}^2}{\eta_{\mathrm{m}}}\left[\frac{p_{\mathrm{i}}}{s}-\left(\frac{R_{\mathrm{m}}^2\mu Q_{\mathrm{m}}}{2k_{\mathrm{m}}\rho}\right)\frac{I_0(r_{\mathrm{D}}\sqrt{s})}{s\sqrt{s}I_1(\sqrt{s})}\right]$	$\frac{R_{\mathrm{m}}^2}{\eta_{\mathrm{m}}}\left[\frac{p_{\mathrm{i}}}{s}-\left(\frac{R_{\mathrm{m}}^2\mu}{2k_{\mathrm{m}}\rho}\right)\frac{Q_{\mathrm{m}}}{s^2}\right]$

Table IV. Matrix pressure and its average in spherical matrix block for different boundary conditions

Matrix and fracture BC	P_{m}	$\overline{P}_{\mathrm{m}}$
Constant pressure p_{f}	$\frac{R_{\mathrm{m}}^2}{\eta_{\mathrm{m}}}\left[\frac{p_{\mathrm{i}}}{s}+\frac{(p_{\mathrm{f}}-p_{\mathrm{i}})}{s}\frac{1}{r_{\mathrm{D}}}\frac{\sinh(r_D\sqrt{s})}{\sinh\sqrt{s}}\right]$	$\frac{R_{\mathrm{m}}^2}{\eta_{\mathrm{m}}}\left[\frac{p_{\mathrm{i}}}{s}+\frac{(p_{\mathrm{f}}-p_{\mathrm{i}})}{s}\frac{3}{\sqrt{s}}\left\{\coth\sqrt{s}-\frac{1}{\sqrt{s}}\right\}\right]$
Linear decline, $p_{\mathrm{f}}=p_{\mathrm{i}}(1-\alpha t)\alpha\leqslant 1/t$	$\frac{R_{\mathrm{m}}^2}{\eta_{\mathrm{m}}}\left[\frac{p_{\mathrm{i}}}{s}-\frac{p_{\mathrm{i}}}{s^2}\frac{\alpha}{\sqrt{s}}\frac{1}{r_{\mathrm{D}}}\frac{\sinh(r_{\mathrm{D}}\sqrt{s})}{\sinh\sqrt{s}}\right]$	$\frac{R_{\mathrm{m}}^2}{\eta_{\mathrm{m}}}\left[\frac{p_{\mathrm{i}}}{s}-\frac{p_{\mathrm{i}}}{s^2}\frac{3\alpha}{\sqrt{s}}\left(\coth\sqrt{s}-\frac{1}{\sqrt{s}}\right)\right]$
Exponential, $p_{\mathrm{f}}=p_{\mathrm{i}}\mathrm{e}^{-\alpha t}$	$\frac{R_{\mathrm{m}}^2}{\eta_{\mathrm{m}}}\left[\frac{p_{\mathrm{i}}}{s}-\frac{p_{\mathrm{i}}}{\sqrt{s}}\left(\frac{1}{s}-\frac{1}{s+\alpha}\right)\frac{1}{r_{\mathrm{D}}}\frac{\sinh(r_{\mathrm{D}}\sqrt{s})}{\sinh\sqrt{s}}\right]$	$\frac{R_{\mathrm{m}}^2}{\eta_{\mathrm{m}}}\left[\frac{p_{\mathrm{i}}}{s}-\frac{3p_{\mathrm{i}}}{s\sqrt{s}}\left(1-\frac{s}{s+\alpha}\right)\left(\coth\sqrt{s}-\frac{1}{\sqrt{s}}\right)\right]$
Constant flux, Q_{m}	$\frac{R_{\mathrm{m}}^2}{\eta_{\mathrm{m}}}\left[\frac{p_{\mathrm{i}}}{s}-\frac{R_{\mathrm{m}}^2\mu Q_{\mathrm{m}}}{3k_{\mathrm{m}}\rho}\frac{3\sinh(r_{\mathrm{D}}\sqrt{s})}{s\left(\cosh\sqrt{s}-\frac{1}{R_{\mathrm{m}}}\sinh\sqrt{s}\right)}\right]$	$\frac{R_{\mathrm{m}}^2}{\eta_{\mathrm{m}}}\left[\frac{p_{\mathrm{i}}}{s}-\left(\frac{R_{\mathrm{m}}^2\mu}{3k_{\mathrm{m}}\rho}\right)\frac{Q_{\mathrm{m}}}{s^2}\right]$

Results

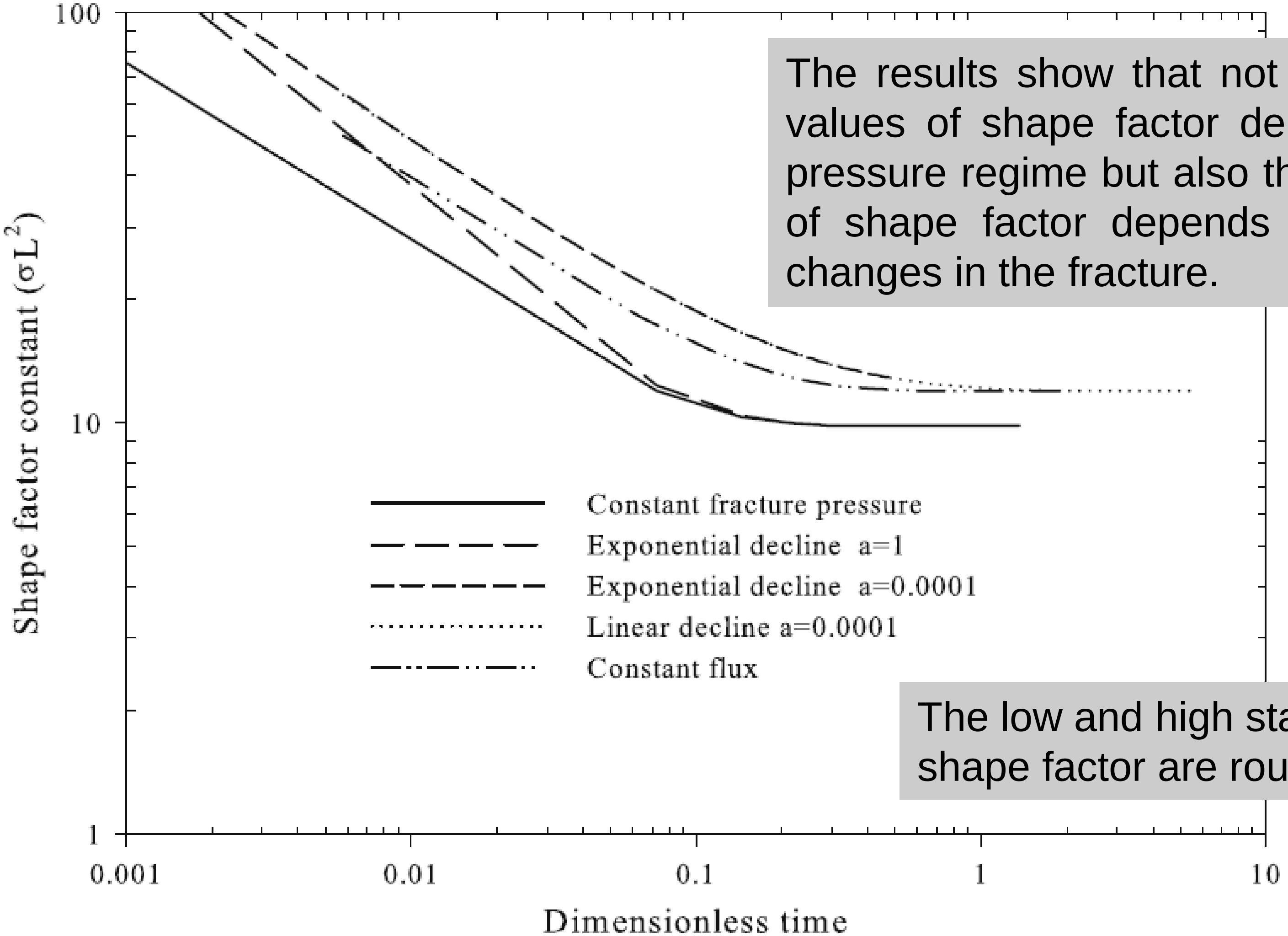

The results show that not only the transient values of shape factor depends on fracture pressure regime but also the late time values of shape factor depends on how pressure changes in the fracture.

The low and high stabilized values of shape factor are roughly 20% apart.

Figure 1. Shape factor constant for slab shape matrix block subject to different boundary conditions.

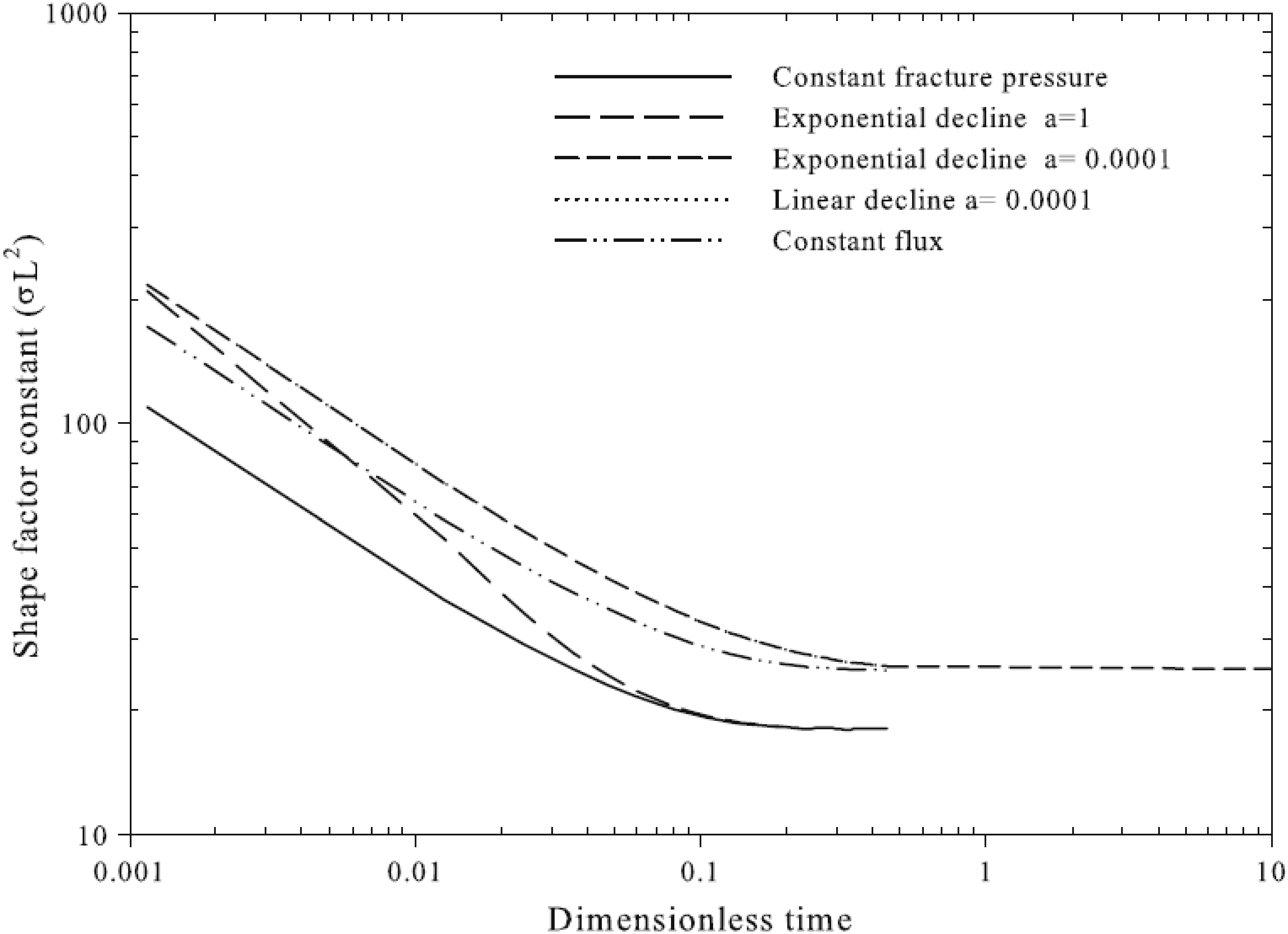

Figure 2. Shape factor constant for cylindrical shape matrix block subject to different boundary conditions.

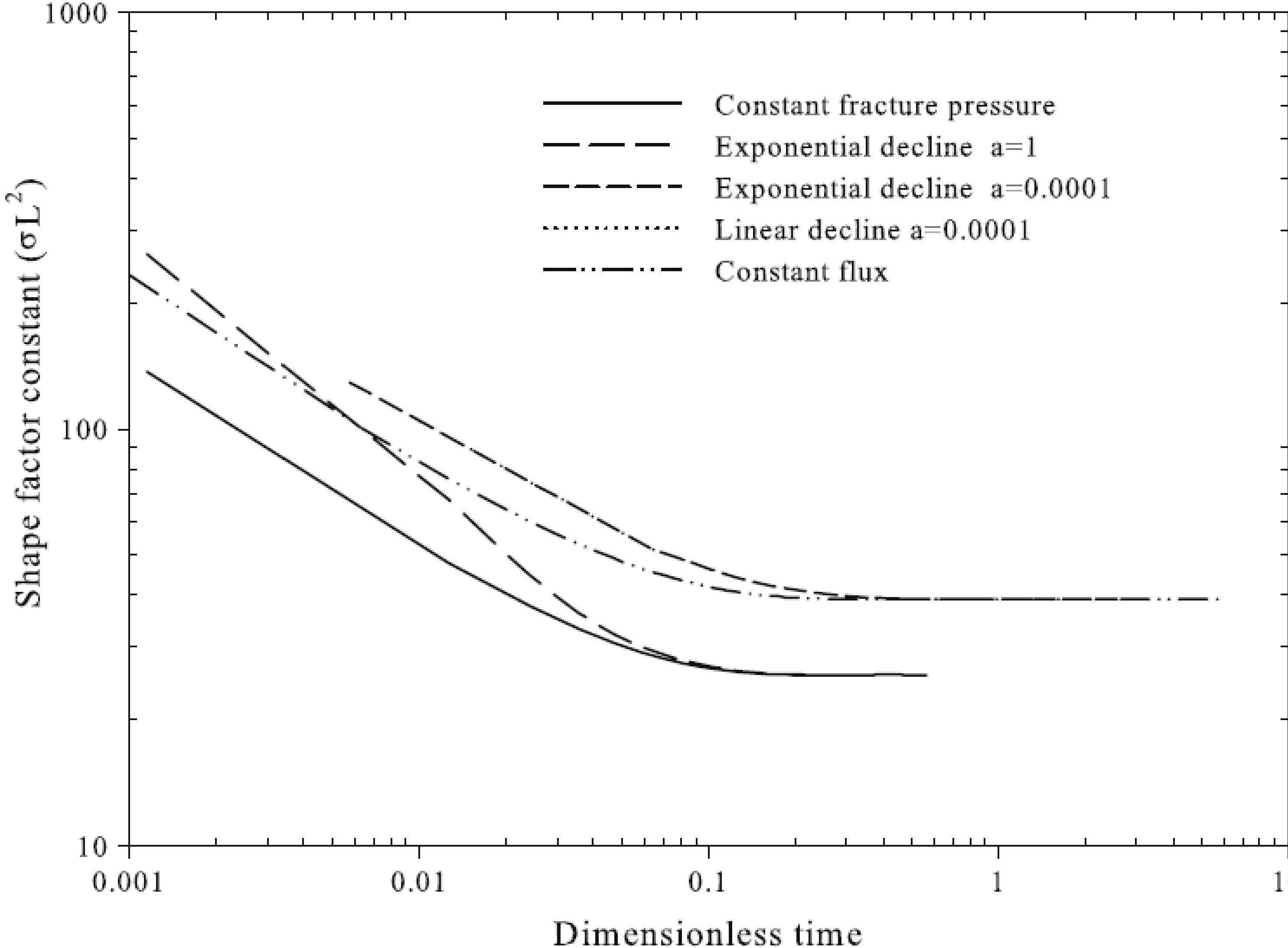

Figure 3. Shape factor constant for spherical shape matrix block subject to different boundary conditions.

Significance of the Results

- It is found that depending on the boundary condition two stabilized shape factor constant can be obtained for each geometry, which could be 20–40% apart.
- Results also reveal that the time to stabilization depends on the boundary condition imposed on the matrix block.
- It was shown in Figures 1–3 that the different stabilized values can be obtained by applying an exponential boundary condition with various **a** exponents, where large values of the exponent give the smaller stabilized value of the shape-factor constant.

Table V. Shape factor constant for different geometry matrix block subject to different boundary conditions

Type of boundary condition	Shape factor constants, σL^2		
	Slab	Cylindrical	Spherical
Constant fracture pressure	9.87	18.2	25.65
Exponential, $a = 1$	9.87	18.2	25.65
Exponential, $a = 0.0001$	12	25.13	39
Linear, all a	12	25.5	39
Constant flux	12	25.13	39

- The stabilized value of the shape-factor constant is usually used in the traditional double porosity model. This can cause the following two types of errors:
  (1) the matrix-fracture transfer would be underestimated at early times, because Figures 1–3 show that at early times, the actual value of shape-factor constant is larger than the stabilized value.
  (2) Depending on the stabilized value of the shape factor chosen, the calculated value could be significantly different even at late times.

What is the magnitude of the error if one uses the stabilized value of shape factor instead of its transient value?

- The relative errors as the difference between the flow rates as calculated using the transient shape-factor and the stabilized-shape factor divided by the rate using the transient-shape factor.

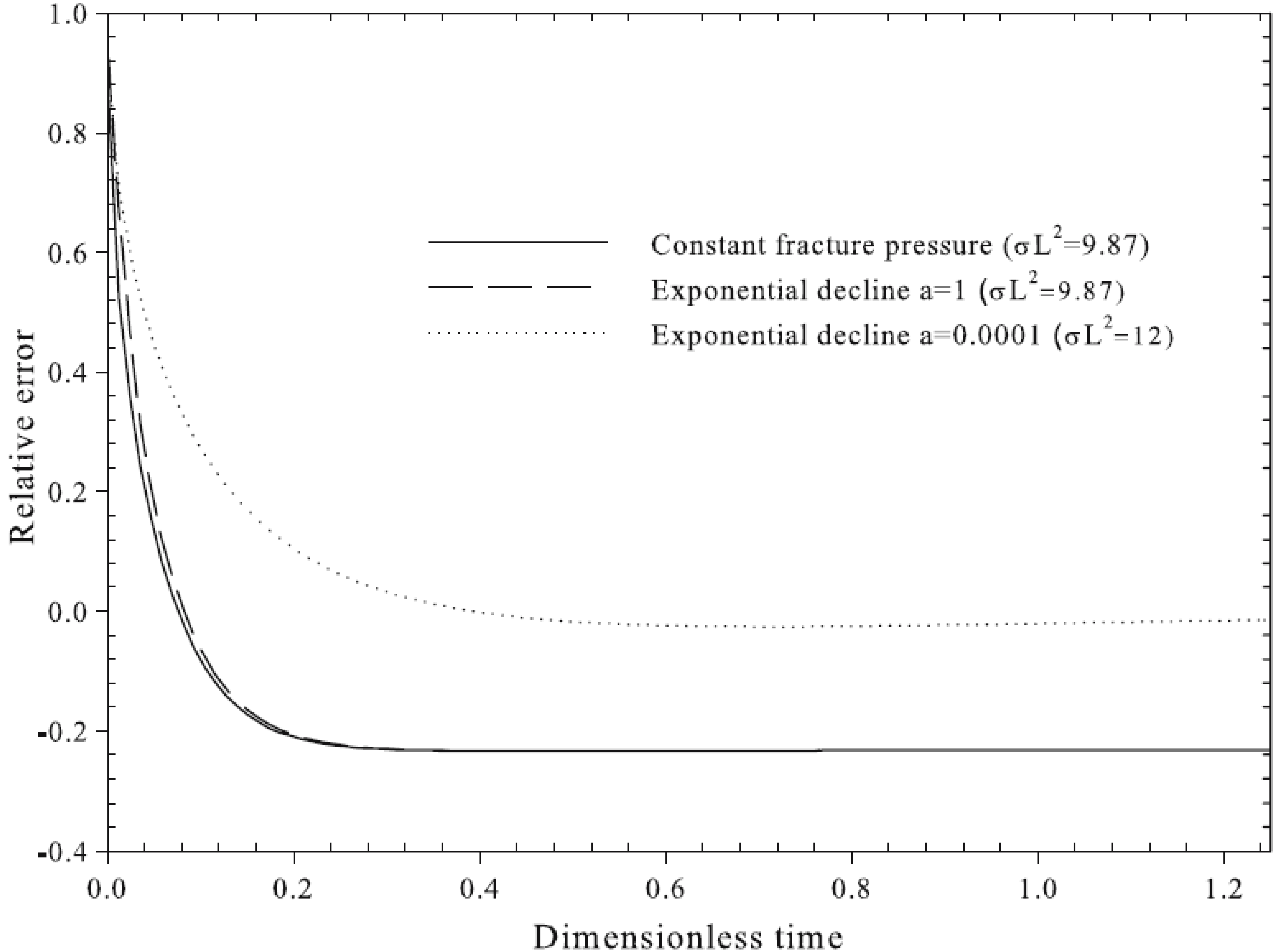

Figure 4. Relative error for a slab shape matrix block subject to different boundary conditions.

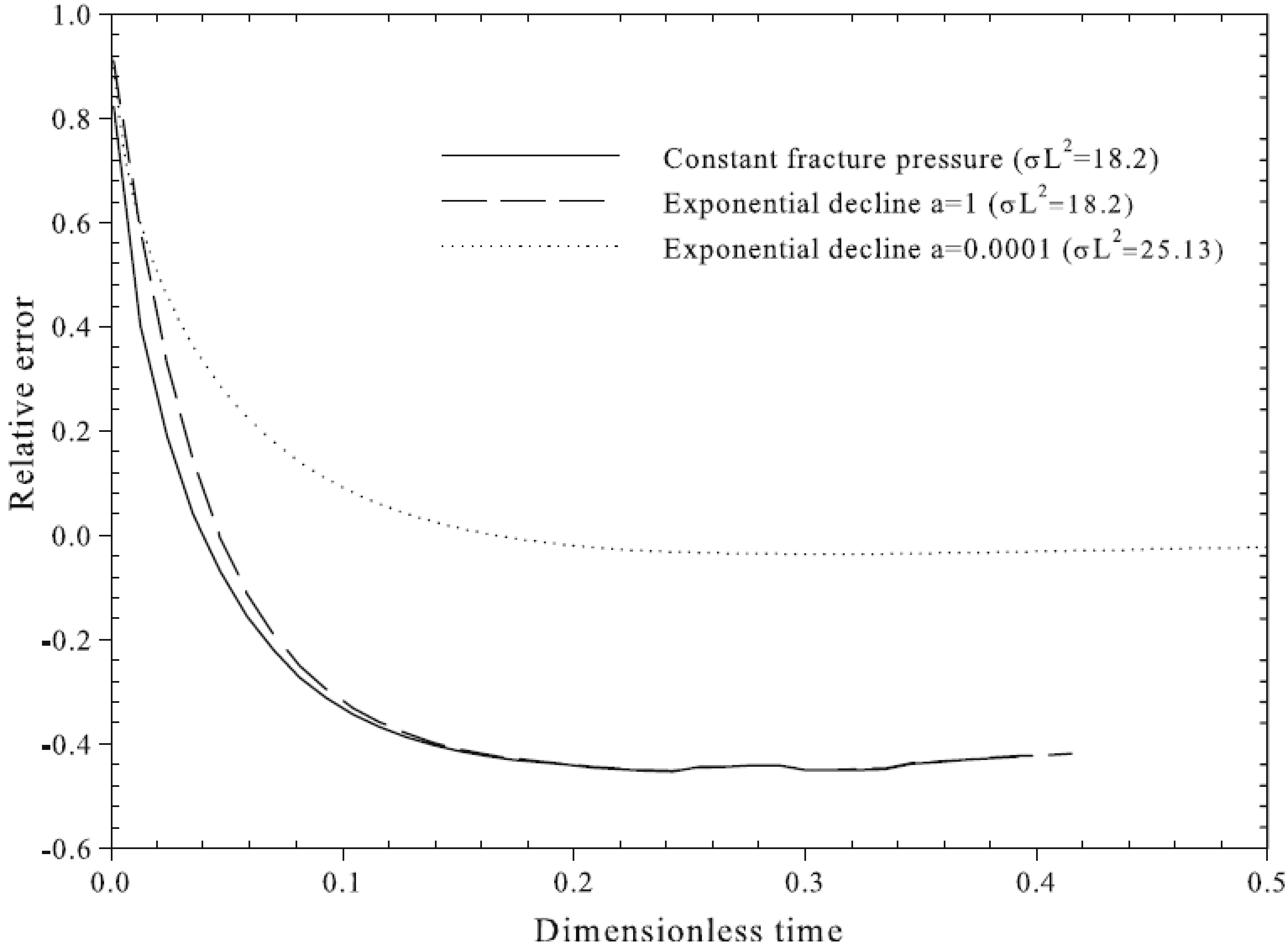

Figure 5. Relative error for a cylindrical shape matrix block subject to different boundary conditions.

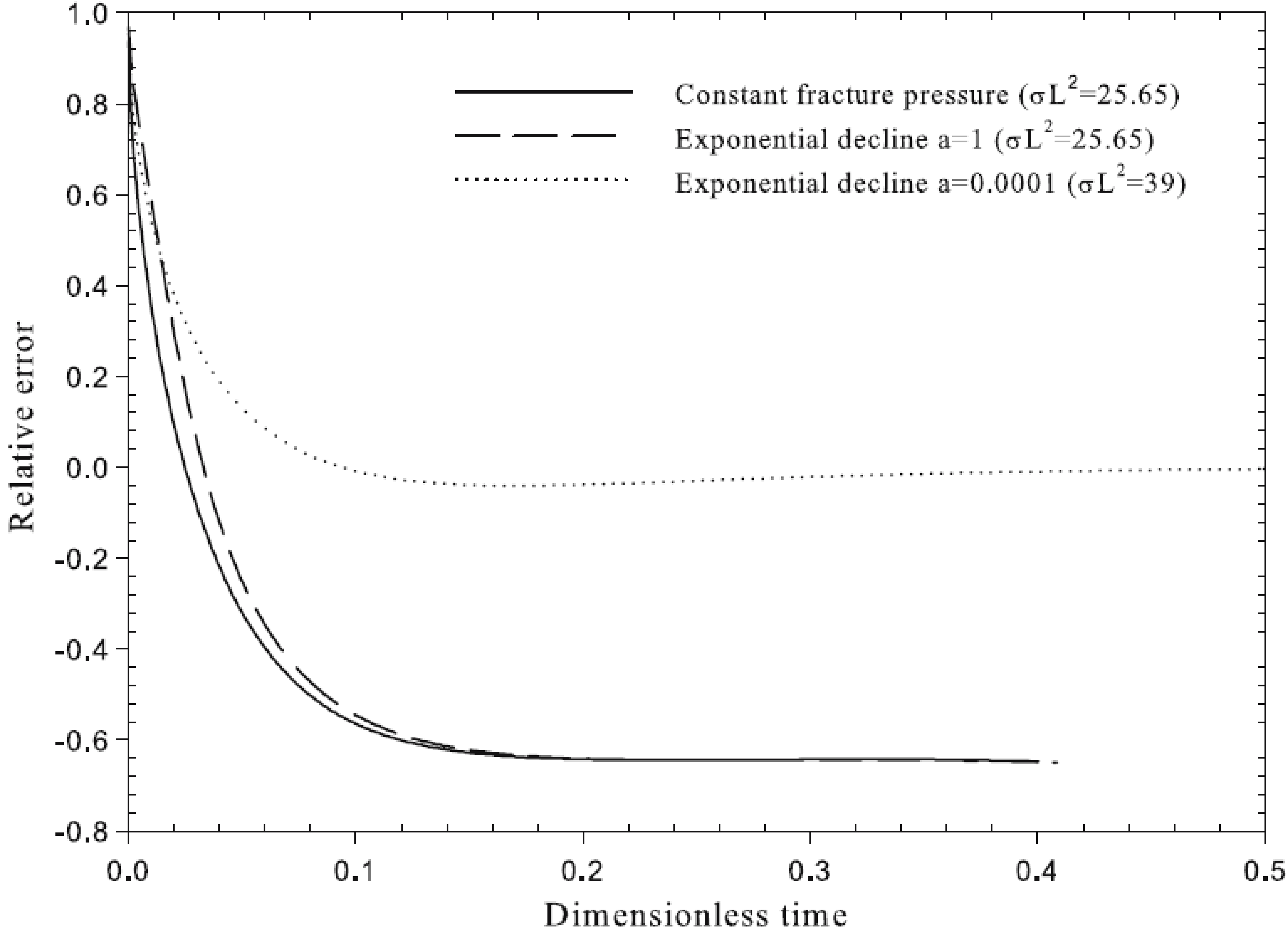

Figure 6. Relative error for a spherical shape matrix block subject to different boundary conditions.

Time Variability of Boundary Conditions

➢The time variability of boundary conditions can be accounted for by using the Duhamel's theorem.

➢In theory a linear pressure decline in the fracture can be modeled by an infinite number of infinitesimal step changes and application of the Duhamel's theorem to calculate the pressure and fluid efflux.

$$Q_{\mathrm{m}} = \frac{k_{\mathrm{m}}\rho}{\mu}\sigma\left(\overline{p}_{\mathrm{m}} - p_{\mathrm{f}}\right), \qquad (1)$$

$$q_{\mathrm{m}} = \int_0^t \frac{\partial \Delta P_{\mathrm{f}}}{\partial \tau}\, q(t-\tau)\, d\tau$$

$$Q_{\mathrm{m}} = -\phi_{\mathrm{m}} c_{\mathrm{m}} \rho \left(\frac{\partial \overline{p}_{\mathrm{m}}}{\partial t}\right), \qquad (2)$$

Using Equations (1) and (2) assuming the matrix block behaves as a lumped system, the pressure change in the matrix block can be described by the following ordinary differential equation

$$\frac{d\bar{p}_m}{dt} + \gamma \bar{p}_m = \gamma p_f \qquad (15)$$

where $\gamma = k_m \sigma / \mu \phi_m c_m$ (16)

We solve the above problem using Duhamel's theorem and its stepwise approximation and compare the solutions. Solution for this ODE for constant and linear ($p_f = p_i(1 - \alpha' t_D), \alpha' \leq 1/t_D$) fracture pressure are given by the following equations, respectively.

$$\bar{p}_m(t_D) = p_f + \left(p_i - p_f\right) e^{-\left(\frac{\pi^2}{4}\right)t_D} \quad \text{(constant fracture pressure)} \tag{17}$$

$$\bar{p}_m(t_D) = p_i \left\{(1 - \alpha' t_D) + \frac{4\alpha'}{\pi^2}\left(1 - e^{-\frac{\pi^2}{4}t_D}\right)\right\} \quad \text{(linear fracture pressure)} \tag{18}$$

The average matrix pressure and fluid efflux for a linear fracture pressure can be obtained by superposition of the constant fracture pressure solutions.

Conclusions

- The matrix-fracture transfer shape factor depends on the pressure regime in the fracture and how it changes with time. Depending on the pressure regime in the fracture a range of stabilized values can be obtained. The upper value is obtained from a slow (linear or exponential) pressure depletion in the fracture and the lower bound by a fast depletion in the fracture.

- The time variability of the fracture boundary condition can be accounted for by the superposition solution of the constant fracture pressure only through a large number of pressure steps.

- The boundary condition dependency of a shape factor can be characterized by applying an exponential-decline boundary condition with varying decline exponents, where fast declines lead to a smaller value of the shape-factor constant. A range of shape factors can be obtained by assigning different exponents.

- It is shown that using the stabilized shape factor introduces large errors in the rate of matrix-fracture transfer by fluid expansion at early and late times.

- For single-phase flow applications, using the shape factor is meaningful when it is derived based on an appropriate geometry, physics, and boundary conditions.

Appendix
Duhamel's Theorem

Superposition

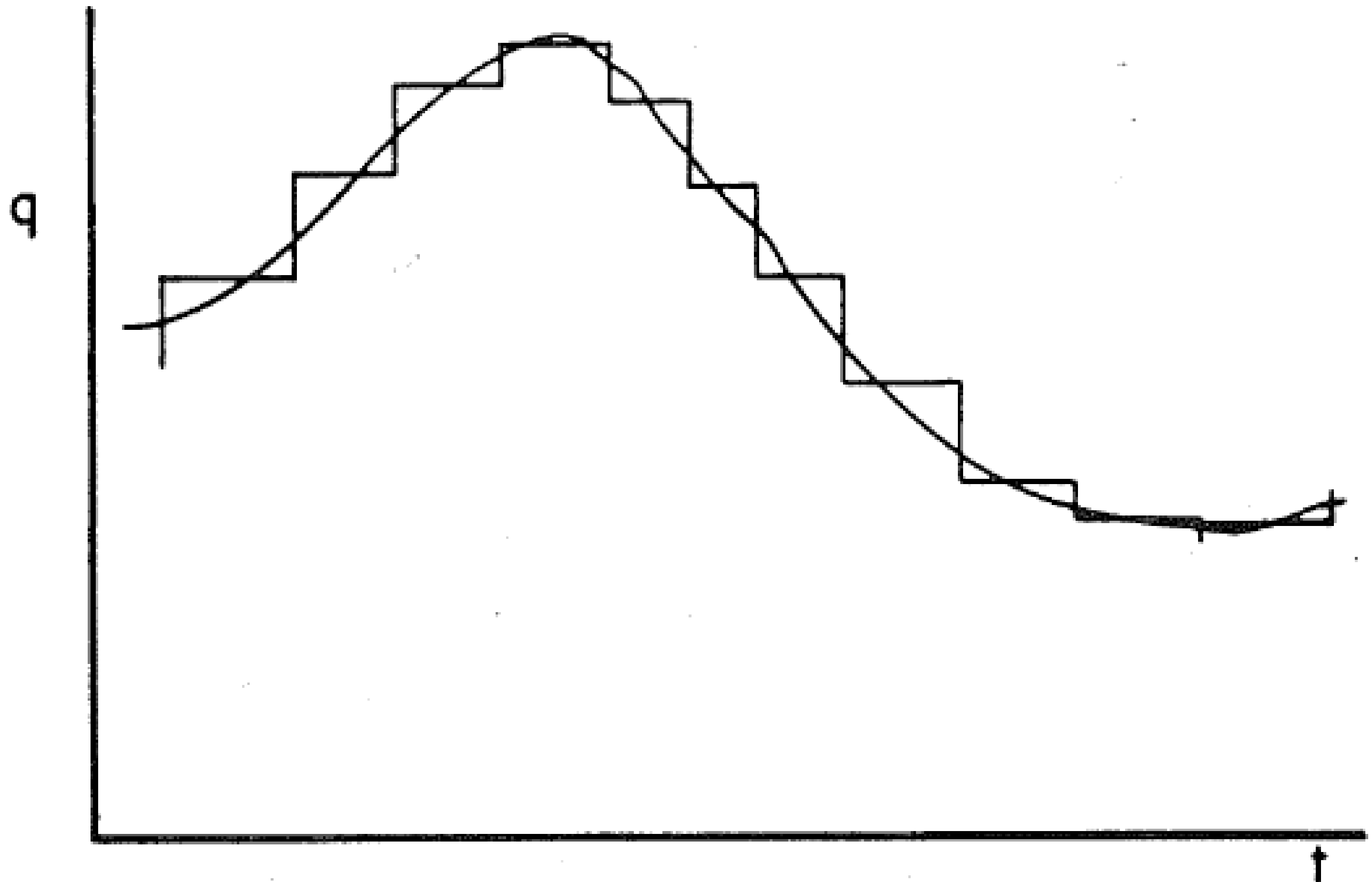

Figure 3-5. Hypothetical case of varying q versus time.

$$
\left.
\begin{aligned}
\text{Let} \quad q_0 &= 0 \text{ and } t_0 = 0 \\
q_1 &= \text{the mean flow rate from } t = 0 \text{ to } t = t_1 \\
q_2 &= \text{the mean flow rate from } t = t_1 \text{ to } t = t_2 \\
q_3 &= \text{the mean flow rate from } t = t_2 \text{ to } t = t_3 \\
&\vdots \\
q_{n-1} &= \text{the mean flow rate from } t = t_{n-2} \text{ to } t = t_{n-1} \\
q_n &= \text{the mean flow rate from } t = t_{n-1} \text{ to } t = t_n
\end{aligned}
\right\} \quad (3\text{-}5)
$$

Also let $m' = \dfrac{162.6\, B_o\, \mu}{k\, h}$

then, Equation 1-22 can be superposed as follows:

$$
\begin{aligned}
\Delta P_1 &= m'\, q_1 \left[\log t_n + \bar{s}\right] \\
\Delta P_2 &= -\, m'\, (q_1 - q_2) \left[\log (t_n - t_1) + \bar{s}\right] \\
\Delta P_3 &= -\, m'\, (q_2 - q_3) \left[\log (t_n - t_2) + \bar{s}\right] \\
&\vdots \\
\Delta P_n &= -\, m'\, (q_{n-1} - q_n) \left[\log (t_n - t_{n-1}) + \bar{s}\right]
\end{aligned}
$$

The sum $\Delta P = P_i - P_{wf}$ is given by:

$$\frac{P_i - P_{wf}}{q_n} = m' \frac{1}{q_n}\left\{[(q_1 - q_0) \log (t_n - t_0) + (q_2 - q_1) \log (t_n - t_1) + (q_3 - q_2) \log (t_n - t_2) + \ldots + (q_n - q_{n-1}) \log (t_n - t_{n-1})]\right\} + m' \bar{s} \qquad (3\text{-}6)$$

Equation 3-6 is the multirate flow equation. In this equation, the rate-time function, RTF, is defined by:

$$RTF = \frac{1}{q_n}\left[(q_1 - q_0) \log (t_n - t_0) + (q_2 - q_1) \log (t_n - t_1) + (q_3 - q_2) \log (t_n - t_2) + \ldots + (q_n - q_{n-1}) \log (t_n - t_{n-1})\right] \qquad (3\text{-}7)$$

According to Equation 3-6, a plot of $(P_i - P_{wf})/q_n$ versus RTF is a straight line of slope m' and intercept equal to $m' \bar{s}$, from which s is determined.

Equation 3-6 can also be expressed as follows:

$$\frac{P_i - P_{wf}}{q_n} = m' \left[\sum_{j=1}^{n} \frac{1}{q_n} \{(q_j - q_{j-1}) \log (t_n - t_{j-1})\}\right] + m \bar{s} \qquad (3\text{-}6)$$

where $q_0 = 0$

$t_0 = 0$

No Skin

$$\frac{P_i - P_{wf}}{q_n} = m' \sum_{j=1}^{n} \left[\frac{1}{q_n} \frac{dq}{dt} \bigg|_{q_j} \Delta t \log\left(t_n - t_{j-1}\right) \right] \qquad (3\text{-}10)$$

Since for a given n both t_n and q_n are constants, then Equation 3-10 is numerically equivalent to the following equation:

Convolution Integral

$$\frac{P_i - P_{wf}}{q_n} = \frac{m'}{q_n} \int_0^{t_n} \frac{dq}{dt} \log\left(t_n - t\right) dt \qquad (3\text{-}11)$$

It is evident that the multirate drawdown equation (Equation 3-10) was derived by superposition. It has been shown that the convolution integral equation (Equation 3-11) is an equivalent expression of Equation 3-10. Therefore, we conclude that convolution and superposition are the same.

We could write Equation 3-11 as follows:

$$P_i - P_{wf}(t) = m' \int_0^t \frac{dq(\tau)}{d\tau} \log(t-\tau)\, d\tau + m'\, q_n\, \bar{s} \tag{3-11}$$

Since q(t) and log (t) are continuous functions of time, the above equation could also be written as:

$$P_i - P_{wf}(t) = m' \int_0^t \frac{dq(t-\tau)}{d\tau} \log(\tau)\, d\tau + m'\, q_n\, \bar{s}$$

Note that the occurrence of $m' \log(t - \tau)$ and $\bar{s}$ in Equation 3-11 is due to the fact that we have adopted the approximate logarithmic solution to the radial flow Equation 1-26 for a homogeneous, infinite reservoir and constant flow rate. Furthermore, in deriving Equation 3-11 we have assumed that at $t = 0$, $q(0) = 0$.

To generalize Equation 3-11, we first remove the requirement that $q(0) = 0$, and we let $P(t)$ be the *unit influence function*. It is the solution of Equation 1-26, at $r = r_w$, which corresponds to a unit rate of production. Then,

$$\Delta P(0) = q(0)\, P(t)$$

and

$$\Delta P(t_1) = [q(t_1) - q(0)]\, P(t - t_1)$$

$$\Delta P(t_2) = [q(t_2) - q(t_1)]\, P(t - t_2)$$

$$\bullet = \quad \bullet$$

$$\bullet = \quad \bullet$$

$$\Delta P(t_5) = [q(t_5) - q(t_4)]\, P(t - t_5)$$

By superposition, the total pressure drop at the wellbore, $\Delta P = P_i - P_{wf}(t)$, is simply the sum of the above expressions. Thus,

$$\Delta P = q(0)\ P(t) + [q(t_1) - q(0)]\ P(t - t_1) + [q(t_2) - q(t_1)]\ P(t - t_2) + \ldots\ldots\ldots\ldots$$

$$\text{or, } \Delta P = q(0)\ P(t) + \frac{q(t_1) - q(0)}{t_1 - 0}(t_1 - 0)\ P(t - t_1)\ \frac{q(t_2) - q(t_1)}{t_2 - t_1}(t_2 - t_1)\ P(t - t_2) + \ldots\ldots$$

which in the limit becomes:

$$\Delta P = q(0)\ P(t) + \int_0^t \frac{dq(\tau)}{d\tau} P(t - \tau)\ d\tau \qquad (3\text{-}20)$$

We now integrate by parts. Let

$$u = P(t - \tau) \text{ then } du = -\frac{dP(t-\tau)}{d\tau}\, d\tau$$

$$\text{and } dv = \frac{dq(\tau)}{d\tau} \text{ then } v = q(\tau)$$

$$\text{Thus, } \int_0^t \frac{dq(\tau)}{d\tau} P(t-\tau)\, d\tau = q(\tau)\, P(t-\tau)\Big|_0^t + \int_0^t q(\tau) \frac{dP(t-\tau)}{d\tau}\, d\tau$$

$$= q(t)P(0) - q(0)P(t) + \int_0^t q(\tau) \frac{dP(t-\tau)}{d\tau}\, d\tau$$

Equation 3-20 can now be written

$$\Delta P = q(t)P(0) + \int_0^t q(\tau) \frac{dP(t-\tau)}{d\tau}\, d\tau \qquad (3\text{-}21)$$

Let $\Delta P_s = P_i - P_{wf(obs)}$

then, when $q(0) = 0$, Equation 3-20 becomes

$$\Delta P_s = \int_0^t \frac{dq(\tau)}{d\tau} P_s(t - \tau)d\tau \qquad (3\text{-}22)$$

Since $q(t)$ and $P_s(t)$ are continuous functions of t, the following result applies to all the convolution integrals:

$$\int_0^t q(\tau) \frac{dP_s(t - \tau)}{d\tau} d\tau = \int_0^t q(t - \tau)\frac{dP_s(\tau)}{d\tau} d\tau$$

Duhamel's Theorem- Variable Rate

$$\Delta P_s = \int_0^t \frac{dq(\tau)}{d\tau} P_s(t-\tau)d\tau$$

Duhamel's Theorem- Variable Pressure

$$q_m = \int_0^t \frac{\partial \Delta P_f}{\partial \tau} q(t-\tau)\, d\tau$$